

TROPICAL PACIFIC OCEAN LONG WAVES CONTRIBUTION TO LENGTH OF DAY DURING ENSO IN 1980-1997

Rodrigo J. Abarca del Rio,¹ Boris Dewitte,¹ Yves duPenhoat¹ and Daniel Gambis²

¹LEGOS-GRGS-UMR5566, 18 Av E d Belin, 31400 Toulouse, France

²IERS, Paris Observatory, URA1125, 61 Av de l'Observatoire, 75014 Paris, France

1. INTRODUCTION

Theoretical studies showed in the early 80s that the low frequency variability associated with ENSO in the tropical Pacific ocean could be explained to a large extent by the contribution of long wavelength equatorial waves (Cane and Sarachik, 1981; Cane, 1984). Such predictions were only confirmed for the whole basin about 10 years later from observations, in particular, from altimetry. Thus, several authors used sea level data derived from satellite measurements to estimate the Kelvin and Rossby wave contributions in the tropical Pacific ocean (Delcroix et al., 1994; Boulanger and Menkes, 1995; Périgaud and Dewitte, 1996 [hereafter PD96]) and showed that they could explain to a large extent the observed thermocline displacements and zonal current low frequency variability.

Whereas the classical delayed oscillator theory (Schopf and Suarez, 1988) considers that the main source (sink) of heat during El Niño (La Niña) is due to the deepening (rising) of the thermocline depth in the eastern Pacific, recent studies have highlighted the importance of zonal advection in displacing the warm pool (Picaut and Delcroix, 1995) and consequently in warming or cooling of the eastern Pacific during ENSO (Picaut et al., 1997). This zonal displacement of a huge water mass associated with the oceanic zonal current raises the question of its impact on the Earth's length of day (LOD), which has been shown to have interannual variations similar to El Niño since Stefanick (1982) and Chao (1984). Although the main share of the signal in LOD at interannual frequencies can be attributed to zonal winds variations (Eubanks, 1993), the study at these time scales of the effect of oceanic zonal currents, and especially the equatorial ocean variability has, for instance, not been undertaken and deserves special attention.

We propose in this study to estimate from the analysis of sea level observations the contribution of the interannual variability of the equatorial Pacific ocean to global angular momentum and to compare it to LOD and atmospheric angular momentum (AAM). We take advantage of a technique used to derived zonal current anomalies from sea level variations (PD96; Dewitte, 1998). Expendable Bathythermograph (XBT) measurements are used as a proxy of sea level over 1980-1998. Sea level data derived from TOPEX/POSEIDON are also used over the period September 1992-May 1998. We first present the data sets and briefly detail the computations and assumptions realized in the study. The last section is devoted to the analysis of the results.

2. DATA AND COMPUTATIONS

The XBT data set was provided by N. Smith from Bureau of Meteorology Research Center (see Smith et al. [1995]). Thermocline depth anomalies are estimated from the ocean heat content in the upper 400 meters as described in PD96. They are further converted into sea level anomalies assuming that the averaged thermocline depth is 150m and that the ocean vertical structure can be approximated to the first baroclinic mode. This latter assumption is necessary to carry on the computation (see PD96) and is to a large extent acceptable for the tropical Pacific (Zebiak and Cane, 1987). Anomalies are relative to the mean over the period January 1982-December 1995. Sea level anomalies are also derived from TOPEX/POSEIDON

measurements (provided and pre-processed by the University of Texas) over the period September 1992-May 1998. Anomalies are relative to the mean over the period January 1993-December 1996.

The length of day (LOD) data from January 1982 to December 1997 on a mean monthly basis was provided by IERS. The AAM data over the same time-span, up to 10 hPa, also on monthly means were computed from four time daily series derived from the reanalyses of NCEP/NCAR (Kalnay et al., 1996) from 1982 to 1983, as from JMA (Japan Meteorological Agency) daily AAM series from 1983 to 1997. Both series were provided by the Atmospheric Special Bureau for the Atmospheres of the IERS established jointly by AER and NOAA (Salstein et al., 1993). Before being compared to the Oceanic Angular Momentum (OAM) series the LOD and AAM series are seasonally filtered using the well-known X11 seasonal filter (Schip and Stier, 1995). Therefore in both series intraseasonal and interannual variability is kept.

Following PD96, sea level anomalies are projected at each longitude onto the meridional structures associated with the first baroclinic mode. The contributions of the Kelvin and the first meridional Rossby modes are derived. The surface baroclinic zonal current anomalies are reconstructed. For the TOPEX period, they differ very little from another estimation using a different technique (Delcroix et al., 1998). The vertical structure of currents and the phase speed are obtained from the vertical mode decomposition of an averaged equatorial density profile taken from a forced OGCM simulation of the tropical Pacific (Dewitte et al., 1998). The mean stratification of this simulation is in very good agreement with the Levitus data set at the equator, which would provide similar results for the first baroclinic vertical structure. The vertical structure is made zonally varying depending on the local stratification to take into account that the thermocline is tilted from west to east. Thus a measure of the overall strength of the zonal anomalous circulation in the equatorial Pacific is given by the relative oceanic angular momentum (OAM) about the rotation axis relative to Earth's surface

$$OAM = \frac{R^3}{g} \int_{x_1}^{x_2} \int_{y_1}^{y_2} \int_{z_1}^{z_2} u(x,y) \cdot F(x,z) \cos^2(y) dx dy dz$$

where R is the radius of the Earth, g the acceleration due to gravity, $u(x,y)$ the surface zonal current anomalies, $F(x,z)$ the first baroclinic mode vertical structure, with the integral performed between $x_1=140^\circ\text{E}$ and $x_2=270^\circ\text{E}$, $y_1=10^\circ\text{S}$ and $y_2=10^\circ\text{N}$, and $z_1=0\text{m}$ and $z_2=600\text{m}$. Note that for $z_2 > 600\text{m}$, $F(x,y)$ is very small and OAM is almost unchanged if the integration is performed up to the ocean bottom.

3. THE RESULTS

Figure 1A presents the difference between LOD and AAM (LOD-AAM). The residual presents intraseasonal and important quasibiennial and quadrennial periods (spectra not shown). Figure 1B presents the OAM anomaly from seasonal climatology time series derived from the XBT and TOPEX data. The OAM series are the total variability from both Kelvin and Rossby waves, but with the Kelvin waves contributing up to 80% of the total variance (not shown). The OAM time series is characterized by a large interannual variability associated with ENSO because the derived zonal current anomalies are themselves strongly correlated to ENSO (Delcroix et al., 1994, DP96). The residual and OAM anomalies are on the same order of magnitude, suggesting that the tropical Pacific Ocean contributes significantly to the closure of the global oceanic angular momentum budget. This is consistent with a recent study based on model outputs (Marcus et al., 1998). To get rid of the intraseasonal variability that is much larger in the atmosphere than in the ocean and in order to extract contributions to the interannual variability in the quasibiennial and quadrennial time scales, we respectively band pass the series on two frequency bands: 1.2 to 2.8 years and 2.8 to 5 years. The results are

presented respectively in the OAM series in Figure 1C and Figure 1D, and they are compared with the residual between the LOD and AAM series there.

The amplitude is on the same order of magnitude for both frequency bands, with a correlation at the 45% level (above the 90% level of significance) for the quasibiennial signals (Figure 1C). Of particular interest is the main agreement of both curves during El Niño 1997. Although the curves are generally slightly phase shifted over 1982 to 1986, they are often in phase after. The main reason for this may be due to that the XBT data prior to 1986 are quite sparse and this results in a larger uncertainty onto the derived zonal current anomalies.

The agreement of the amplitudes is encouraging, mostly because the OAM is here only computed from latitudes going from 15°S to 15°N. Therefore the quasibiennial oscillation in OAM must have a significant variability along the equator. Consequently in the quadrennial band an important variability must also arise from the tropics.

Figure 1B presents also the OAM calculated using the availability of high quality TOPEX/Poseidon satellite measurements of sea level variability. Over the overlapping period (September 1992 to December 1997), both signals are highly correlated, encouraging to use XBT data for OAM computation.

4. CONCLUSIONS

The contribution of the equatorial Pacific low frequency current variability to the global angular momentum of the Earth-atmosphere-ocean system was estimated from observations. Although LOD and AAM at interannual time scales are highly correlated, their difference presents quasibiennial and quadrennial periods. The oceanic angular momentum calculated from the equatorial Pacific Ocean is shown to have the same order of magnitude as the LOD-AAM residual. Although other tropical oceans are not considered, their interannual variability is much less and is then unlikely to significantly alter our result. Note also that it is much more difficult to derive zonal current from observations in the other tropical oceans. However although this estimation is largely dependent onto the approximations made to derive the oceanic zonal current anomalies (mostly the one baroclinic mode approximation), the result suggests a large impact of the upper oceanic variability in the tropics associated to ENSO onto the LOD. The correlation at the quasibiennial period is highly promising, since the quasibiennial period plays an important and complex role on LOD at interannual time scales. Although the OAM must be computed using all the oceanic variability, the tropical Pacific Ocean variability is shown here to be playing a dominant role at interannual time scales.

REFERENCES:

- Boulanger, J.-P., and C. Menkes, 1995: Propagation and reflection of long equatorial waves in the Pacific Ocean during the 1992-1993 El Niño. *J. Geophys. Res.*, 100, 25,041-25,059.
- Cane, M. A., and E. S. Sarachik, 1981: The response of a linear baroclinic equatorial ocean to periodic forcing. *J. Mar. Res.*, 39, 651-693.
- Cane, M. A., 1984: Modeling sea level during El Niño. *J. Phys. Oceanogr.*, 14, 1864-1874.
- Chao, B. F., 1984: Interannual length-of-day variation with relation with the Southern Oscillation/El Niño. *Geophys. Res. Lett.*, 11, 541-544.
- Delcroix, T., J.-P. Boulanger, F. Masia, and C. Menkes, 1994: Geosat-derived sea level and surface current anomalies in the equatorial Pacific during the 1986-1989 El Niño and La Niña. *J. Geophys. Res.*, 99, 25,093-25,107.

Delcroix, T., B. Dewitte, Y. duPenhoat, F. Masia, and J. Picaut, 1998: Equatorial waves and warm pool displacements during the 1992-1997 El Niño events. Submitted to *J. Geophys. Res.*

Dewitte, B., G. Reverdin, and C. Maes, 1998: Vertical structure of an OGCM simulation of the tropical Pacific in 1985-1995. *J. Phys. Oceanogr.*, in press.

Dewitte, B., 1998: Sensitivity of an intermediate ocean-atmosphere coupled model of the tropical Pacific to its oceanic vertical structure. Submitted to *J. Climate*.

Eubanks, T. M., 1993: Variations in the orientation of the Earth, in *Contributions of space geodesy to geodynamics*, edited by S. D. E., and D. L. Turcotte, 24, American Geophysical Union, Washington, D.C., 1-54.

Kalnay, E., and co-authors, 1996: The NCEP/NCAR 40-Year reanalysis project. *Bull. Amer. Meteor. Soc.*, 77, 437-471.

Marcus, S. L., Y. Chao, J. O. Dickey, and P. Gegout, 1998: Detection and Modeling of nontidal oceanic effects on Earth's Rotation Rate. *Nature*, 281, 1656-1659.

Périgaud, C. and B. Dewitte, 1996: El Niño-La Niña events simulated with Cane and Zebiak's model and observed with satellite or in situ data. Part I: Model data comparison. *J. Climate*, 9, 65-84.

Picaut, J. and T. Delcroix, 1995: Equatorial wave sequence associated with warm pool displacements during the 1986-1989 El Niño-La Niña. *J. Geophys. Res.*, 100, 18393-18408.

Picaut J., F. Masia, and Y. duPenhoat, 1997: An advective-reflective conceptual model for the oscillatory nature of the ENSO. *Science*, 277, 663-666.

Salstein, D. A., D. M. Kann, A. J. Miller, and R. D. Rosen, 1993: The sub-bureau for atmospheric angular momentum of the international earth rotation service: a meteorological data center with geodetic applications., *Bull. Amer. Meteor. Soc.*, 14, 67-80.

Schips, B., and W. Stier, 1995: The Census-X-11 procedure: Theory, assessment and alternatives, 156-O, Swiss Federal Statistical Office, Bern.

Schopf, P. S., and M. J. Suarez, 1988: Vacillations in a coupled ocean-atmosphere model. *J. Atmos. Sci.*, 45, 549-566.

Smith N. R., J. E. Blomley, and G. Meyers, 1995: An improved system for tropical ocean sub-surface temperature analyses. *J. Atmos. Oceanic. Technol.*, 219-256.

Stefanick, M., 1982: Interannual atmospheric angular momentum variability 1963-1973 and the Southern Oscillation. *J. Geophys. Res.*, 87, 428-432.

Zebiak, S. E., and M. A. Cane, 1987: A model El Niño-Southern Oscillation. *Mon. Weather Rev.*, 115, 2262-2278.

FIGURE CAPTIONS:

Figure 1a: Difference between length of day (LOD) and atmospheric angular momentum (AAM). The data have first been seasonally filtered. Unit in Milliseconds (ms).

Figure 1b: Oceanic Angular Momentum (OAM) calculated from XBT data (dashed line) and Topex Poseidon data (solid line). Units in milliseconds (ms).

Figure 1c: Comparison at the quasibiennial band (1.2 to 2.8 years) of LOD-AAM residual (solid line) and OAM from XBT data (dashed line). Units in milliseconds (ms).

Figure 1d: Comparison at the quadrennial band (2.8 to 5 years) of LOD-AAM residual (solid line) and OAM from XBT data (dashed line). Units in milliseconds (ms).

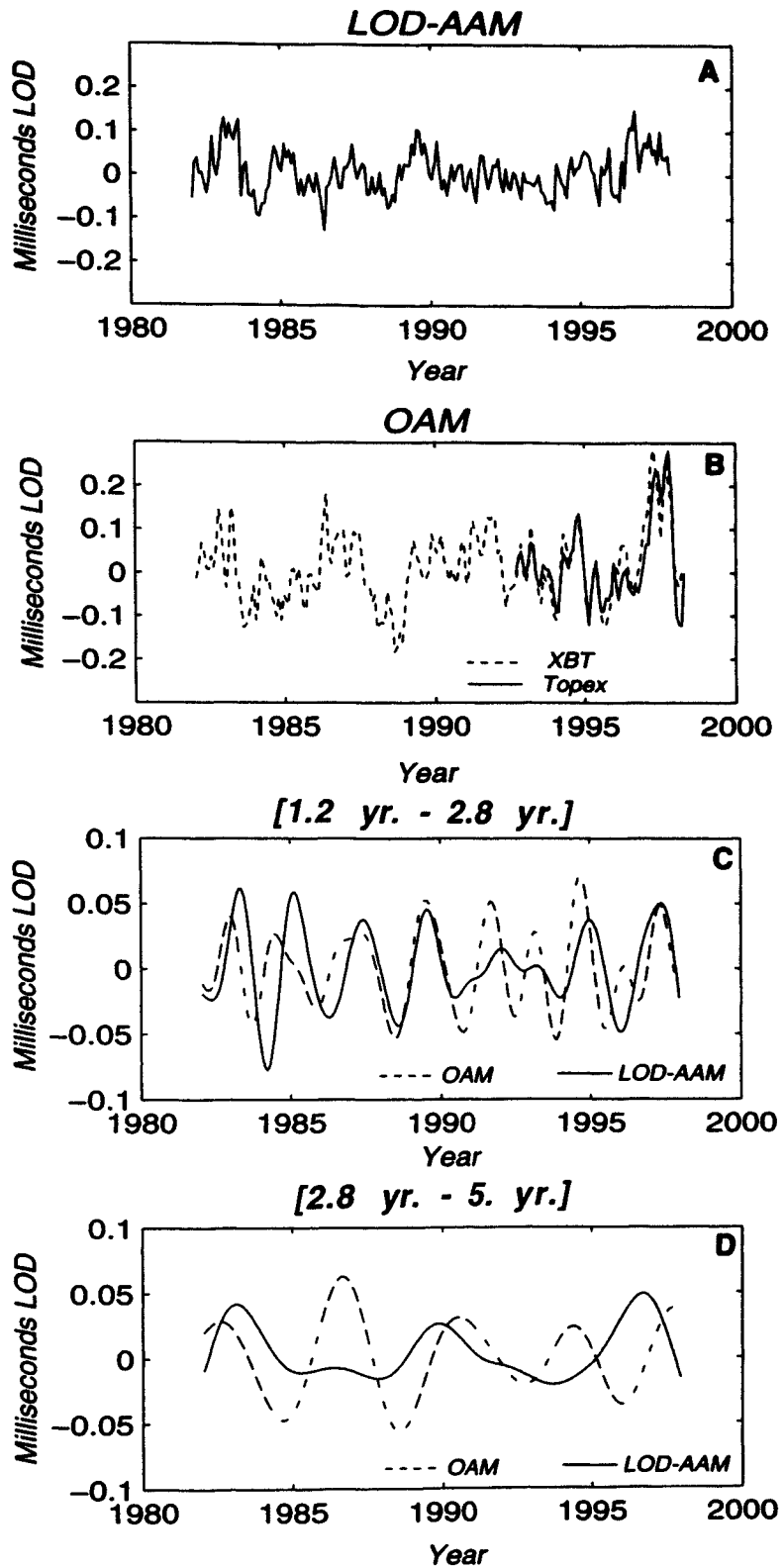


Fig. 1